Holmium-doped fiber amplifier for pumping a ZnGeP₂ optical parametric oscillator

LARS G. HOLMEN[1,2,*] AND HELGE FONNUM[1]

[1]*Norwegian Defence Research Establishment (FFI), Kjeller NO-2027, Norway*
[2]*Department of Technology Systems, University of Oslo, Kjeller NO-2027, Norway*
*lars.holmen@ffi.no

Abstract: We present a holmium-doped all-fiber master oscillator power amplifier (MOPA) system operating at 2108 nm targeting optical frequency conversion applications. The MOPA delivers pulses of 0.52 mJ energy at 10 kHz repetition rate after three amplification stages, with a close to square-shaped temporal profile of 50 ns duration, diffraction-limited beam quality and linear polarization. Challenges with achieving high gain and efficiency in the final amplification stage are discussed and attributed to quenching effects inferred from measurements of non-saturable absorption in the holmium fibers. Using this MOPA, we demonstrate a mid-IR conversion efficiency of 59% by direct pumping of a ZnGeP₂ optical parametric oscillator.

1. Introduction

Rugged and reliable fiber-based laser sources emitting nanosecond-duration pulses with high peak power in the 2 μm spectral range are attractive for applications in remote sensing, material processing, medicine, and defense [1]. Many applications benefit from laser operation somewhat beyond 2 μm, such as free-space optical applications targeting the atmospheric transmission window beyond 2.1 μm. Also, a pump source at 2.1 μm to 2.15 μm is a particularly attractive starting point for nonlinear frequency conversion to the mid-IR, since the generated signal and idler end up in the transmission windows at each side of the 4.2 μm CO_2 absorption band.

One established route for efficient conversion of ∼2 μm radiation to the mid-IR at high average power is pumping of a ZnGeP₂ (ZGP) optical parametric oscillator (OPO), due to attractive features of ZGP including high nonlinearity, good transmission in the mid-IR and good thermal and mechanical properties. ZGP exhibits a defect-related absorption around 2 μm [2], which strongly favors pump wavelengths of 2.1 μm or longer. Traditional ZGP OPOs are often pumped by Q-switched holmium-based solid state lasers such as Ho:YAG, and high performance systems with good beam quality typically achieve conversion efficiencies of 50% to 60%, at tens of watts of mid-IR power [2,3].

Several groups have investigated direct fiber laser pumping of ZGP OPOs [4–8], motivated by the benefits of replacing the traditional solid state pump lasers with efficient and reliable fiber sources with high average power scaling potential. The most basic prerequisite for efficient nonlinear conversion in ZGP is high peak power. Millijoule-level pulses with tens of kW peak power are routinely generated from Q-switched solid state lasers, however such power levels are principally challenging in fiber lasers due to nonlinear effects. The best performance fiber sources currently available in the 2 μm band are based on cladding-pumped thulium-doped fibers. Operation of pulsed Tm-based sources is however challenging for wavelengths above ∼2.05 μm, since high gain pulsed operation favors shorter wavelength emission. Most previous reports of ZGP OPOs pumped by fiber-based sources have nevertheless employed Tm fibers in Q-switched [4,7] or gain-switched [5,6] configurations. As expected from the short operation wavelength around 2.0 μm of these sources, the OPO efficiency and power scaling was hindered by thermal degradation from ZGP absorption.

Compared to thulium, holmium-doped silica fibers have a slightly red-shifted emission spectrum, and can operate naturally in the 2.1 μm to 2.15 μm range [1]. Although holmium fiber laser development is less mature than thulium, some notable 2.1 μm nanosecond-duration sources with properties relevant for ZGP pumping have been demonstrated. A cladding-pumped holmium fiber amplifier seeded by a Q-switched Ho:YAG laser delivered pulses with very high pulse energy (2.25 mJ) and peak power (100 kW), but suffered from severe spectral broadening due to the long gain fiber and high peak power [9]. Another fiber MOPA delivered 99 W of average power in an all-fiber format [10], with pulse energy of 0.6 mJ. These pulses had a relatively long duration, and therefore a peak power below 2 kW. Finally, a core-pumped amplifier based on a custom very large mode area holmium fiber demonstrated 36 kW peak power for 5 ns pulses while maintaining excellent spectral quality [11]. This source was unpolarized, whereas linear polarization would be required for ZGP pumping.

A recently reported ZGP OPO used a co-doped Tm:Ho Q-switched oscillator pump source [8]. This operated at a favorable 2.09 μm wavelength compared to previous OPO demonstrations, and the reported 8.1 W of mid-IR output is currently the highest power demonstration from a fiber laser pumped ZGP OPO. However, the mid-IR conversion efficiency of 24% was only comparable to other reported OPOs, which has been in the range from 15% to the current record of 32% [4]. With the core motivation of fiber laser pumped ZGP OPOs being average power scaling and ultimately bulk laser replacement, it is argued that OPO conversion efficiency is the pressing issue to be addressed for significant progress. Apart from Ref. [7], which was based on a high peak power photonic crystal fiber amplifier, reported pump sources have had relatively low peak powers of a few kW and moderate pulse energies [4–6]. In combination, these aspects are believed to explain the obtained mid-IR conversion efficiencies. Considering the peak power and energy scaling challenges inherent to fiber sources, it is natural to look at source architectures that make the most of the energy and peak power available. One attractive candidate in this regard is a directly diode-seeded master oscillator power amplifier (MOPA), where the agility available in pulse shaping and optimization may to some extent compensate the reduced energy and peak power available for mid-IR conversion relative to bulk pump lasers [12], while retaining the average power scalability inherent to the fiber architecture.

In this work, we present a diode-seeded holmium-doped fiber MOPA tailored for nonlinear conversion applications. The source operates at 2108 nm and delivers pulses with 0.52 mJ pulse energy and 11 kW peak power at 10 kHz repetition rate in a linearly polarized and near-diffraction limited beam. Square pulse shaping is implemented to achieve the highest possible peak power from the fiber source while suppressing the deleterious nonlinear processes of stimulated Brillouin scattering and modulation instability. Despite delivering high quality pulses suitable for optical frequency conversion, the average power scaling of the MOPA is currently hindered by a moderate slope efficiency in the final stage of ~20% with respect to pump power at 1.95 μm. Spectroscopic characterization of the holmium fibers reveals considerable non-saturable absorption that is consistent with the measured efficiency, and may be explained e.g. by clustering of Ho ions and associated pair induced quenching. We finally employ the MOPA for nonlinear frequency generation, and report, to our knowledge, the first ZGP OPO pumped by a singly doped holmium fiber source. The achieved mid-IR conversion efficiency of 59% is substantially higher than previously reported fiber pumped ZGP OPOs, and is for the first time comparable to efficiencies from OPOs pumped by solid state lasers.

2. Experimental setup

The pulsed 2.1 μm fiber source is designed as a master oscillator power amplifier (MOPA) with three amplification stages, illustrated in Fig. 1. The MOPA has an all-fiber architecture with polarization maintaining (PM) fibers and PM fiber-coupled components. The seed oscillator is a single-frequency 2108 nm laser diode (Eblana Photonics), which delivers a peak power

up to ~2 mW. The seed pulses are generated and shaped electronically using a fast arbitrary waveform generator. A pulse repetition rate of 10 kHz is used in this work. Pulse shaping serves two purposes; it precompensates the dynamic gain saturation occurring in the amplifiers, and at the same time imposes a suitable frequency chirp essential for suppressing stimulated Brillouin scattering (SBS). A pulse duration of 50 ns was used, based on the ~0.5 mJ pulse energy and ~10 kW peak power limits that were found for the power amplifier (see Section 3.3.2).
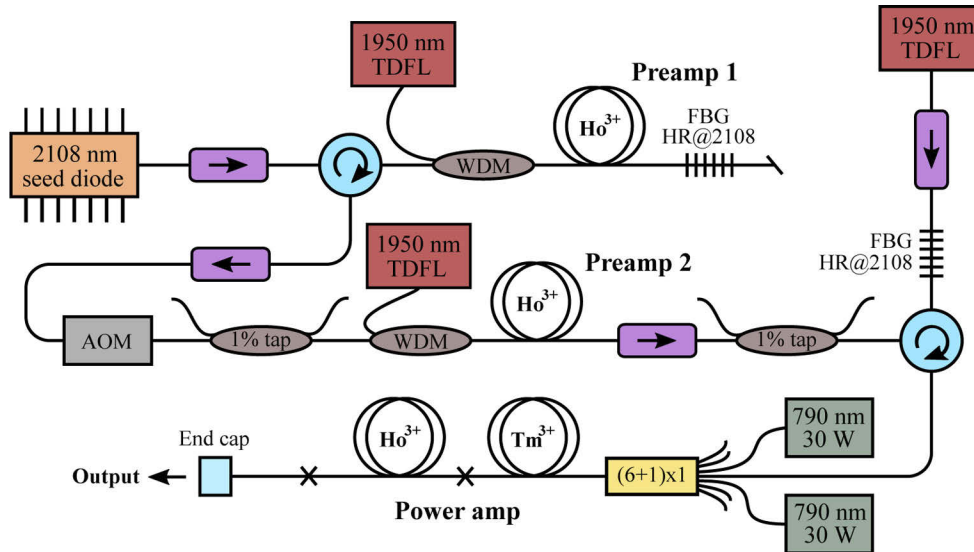

Fig. 1. Illustration of the three-stage fiber amplifier. WDM: wavelength division multiplexer, TDFL: thulium-doped fiber laser, AOM: acousto-optic modulator, HR: highly reflective, FBG: fiber Bragg grating.

The first preamplifier uses a circulator and reflector to achieve high gain double-pass amplification in a 2.5 m long single mode Ho-doped gain fiber (iXblue: IXF-HDF-PM-8-125). The amplifier is pumped at the 1950 nm Ho absorption peak with 2.1 W from a thulium-doped fiber laser (TDFL). The reflector is a highly reflective fiber Bragg grating (FBG) with a 1 nm reflection bandwidth centered at the seed wavelength, which also serves as a spectral filter before the return pass. A fiber coupled acousto-optic modulator (AOM) follows after the first stage, with the purpose of adding dynamic range to the pulse shaping required for generating square output pulses from the final amplifier.

The second preamplifier contains the same components as the first, but the combination of the circulator and FBG is placed after the (single-pass) amplifier to act purely as a spectral filter. A 3.2 m long gain fiber and 2.3 W of 1950 nm pump power is used.

The power amplifier employs a tandem setup with a thulium-doped large mode area (LMA) fiber directly preceding a mode-matched holmium-doped fiber. This in-line setup facilitates core pumping of the Ho fiber at high average powers, without imposing challenging power handling requirements of fiber components otherwise needed to combine the pump and signal. The tandem amplifier is seeded at two wavelengths; the 2108 nm signal from previous stages and ~1 W at 1950 nm from a TDFL launched through the FBG in the final spectral filter. The PM Tm-fiber (iXblue) has a 20 μm core, a 300 μm cladding and a numerical aperture (NA) of 0.08. Pump power from diode lasers at 790 nm is launched through a (6+1)x1 combiner. Holmium-doped LMA fibers from two different manufacturers were tried in the power amplifier, specifically IXF-HDF-PM-20-250 (iXblue) and LMA-HDF-25/250 (Nufern), from here referred to as Fiber X and Fiber N, respectively. Of these, only Fiber X was polarization maintaining, whereas a

PM version of Fiber N was not available. The optimum holmium fiber lengths were determined from cut-back experiments, and resulted in 2.2 m (Fiber X) and 2.3 m (Fiber N). The gain fibers in the power amplifier are mounted on an aluminum plate and loosely coiled at a diameter of ~25 cm. An anti-reflection (AR) coated fused silica bulk end cap is CO_2-laser-bonded to the 0.5 m passive delivery fiber to suppress feedback and prevent catastrophic fiber damage.

3. Results and discussion

3.1. Pulsed seed diode

The measured temporal profile of the pulsed seed diode is shown in Fig. 2(a). The seed pulses are deliberately shaped in order to obtain square output pulses from the power amplifier. Figure 2(b) shows the optical spectrum of the pulsed output, which is spectrally broadened to a 3 dB bandwidth of 0.30 nm (20 GHz), compared to a linewidth of a few MHz in continuous operation. This broadening is attributed to the chirp obtained in semiconductor lasers caused by the carrier density changing with current modulation [13]. The spectral properties of the seed pulses can strongly impact the threshold for stimulated Brillouin scattering (SBS) in the power amplifier, and also influence OPO operation. SBS is expected to be the lowest threshold nonlinear interaction that limits power scaling in a single frequency fiber amplifier with pulse duration above several nanoseconds [14]. Therefore, experiments were done to investigate the instantaneous frequency during the pulses.
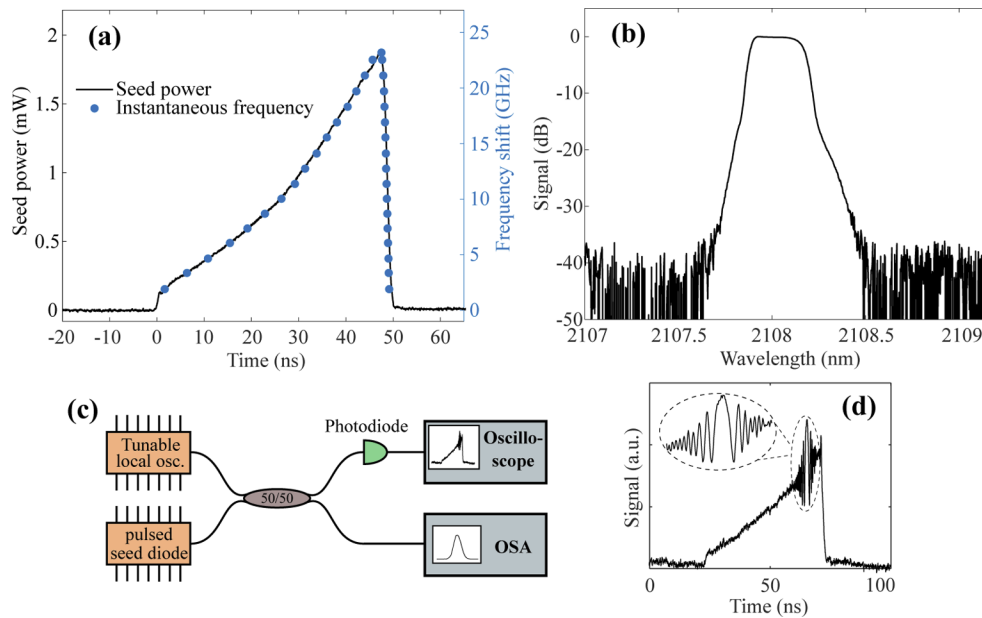

Fig. 2. Measured temporal profile and frequency evolution of the seed pulses (a) and the corresponding optical spectrum with 0.05 nm resolution (b). The heterodyne detection setup used for probing the instantaneous frequency through the pulses is illustrated in (c), and (d) shows an example chirp beat pattern obtained at a particular probe laser wavelength.

The frequency evolution of the seed pulses was characterized with the heterodyne detection setup shown in Fig. 2(c). When mixing the pulsed seed with a tunable diode laser acting as a reference oscillator, an interference beat is obtained with a frequency equal to the difference in optical frequencies. An example of such interference pattern is shown in Fig. 2(d). The finite bandwidth of the detection system (limited by a 1 GHz oscilloscope) precluded use of a single

chirp interference pattern to deduce the full frequency evolution of the pulses. Instead, the full evolution was determined by tuning the reference oscillator across the seed spectrum, while mapping the measured reference wavelength to time instances in the pulse where a zero-frequency crossing was seen in the interference patterns. These results are shown in Fig. 2(a), and reveal a near proportional relationship between the instantaneous power and frequency of the seed output. This agrees with semiconductor laser theory in the case where the frequency is not influenced by thermal effects and predominantly determined by the "adiabatic" frequency chirp [13]. Apparent from Fig. 2(a), the seed laser frequency difference between operation at threshold and peak power is 23.3 GHz, i.e. consistent with the spectral broadening measured with the optical spectrum analyzer.

A numerical analysis was done to estimate the SBS threshold enhancement caused by the spectral broadening of the seed diode by solving the coupled amplitude equations describing the dynamic SBS interaction in the power amplifier [15–17]. When comparing the SBS threshold for 50 ns square pulses having either transform limited bandwidth or the frequency evolution in Fig. 2(a), these simulations suggest thresholds (1% conversion to the Stokes wave) of 60 μJ (1.2 kW) and 3 mJ (61 kW) in the two cases, respectively. In other words, the frequency chirp accompanying the seed pulse shaping is expected to raise the SBS threshold fiftyfold, i.e. to a level where other factors will limit peak power and energy scaling.

3.2. Preamplifiers

3.2.1. High gain double-pass preamplifier

A high gain preamplifier is motivated by the ~70 dB net gain needed to amplify the mW-level peak seed power to the desired 10 kW-regime. The first stage in Fig. 1 addresses this using a double-pass amplification scheme with intra-stage spectral filtering before the return pass. A net gain of 37 dB is realized, which is limited by the onset of parasitic lasing at the FBG wavelength. In essence, the ~425 nW average power from the pulsed seed diode is amplified to 2.3 mW measured after the second isolator. It is noted that the internal performance of the amplifier is better than the external performance due to large insertion losses of fiber-coupled components currently available in this spectral regime. Specifically, the isolators have an insertion loss of 1.0 dB each, the circulator loss is 1.5 dB loss per pass, and the WDM has a 1.0 dB loss per pass at the signal wavelength. Combined, this means that the amplifier operates at an internal gain of 44 dB at 2108 nm.

The preamp design resembles a polarization maintaining version of the holmium fiber amplifiers reported by Simakov et al. [18], which demonstrated excellent performance with high gains up to 40 dB at certain wavelengths in the Ho emission band. One important difference here is the use of a narrowband FBG instead of a broadband reflector for achieving double-pass amplification. This has the drawback of limiting the amplifier to fixed-wavelength operation, but it significantly improves the performance and spectral quality by filtering amplified spontaneous emission (ASE) before the return pass. This reduces the level of out-of-band ASE from the output and removes the need for additional spectral filtering before the second stage. Also, the strong filtering aids the 2108 nm long wavelength operation, which is substantially red-shifted relative to the peak gain of this amplifier (estimated to 2060 nm from ASE spectra).

3.2.2. Second preamplifier

The pulse shaping necessary for adequately compensating the dynamic gain saturation through the whole amplifier chain could not be realized directly from the seed diode, since it would require a period in the beginning of the pulse with a slowly varying seed power (see Fig. 5 for reference). This would imply a small frequency chirp insufficient for SBS suppression. A fiber coupled acousto-optic modulator (AOM) is therefore included between the first and second amplifier to partially decouple the pulse amplitude and spectral shaping. The AOM has a 3.2 dB

insertion loss, hence the seed power entering the second preamplifier is 1.1 mW. The second stage amplifies the signal to 200 mW (measured after the isolator), i.e. a net gain of 22.6 dB. This implies a pulse energy of 200 mW/10 kHz = 20 μJ, and the corresponding peak power of these pulses is ~800 W. Further amplification of these pulses was prevented by the onset of spectral degradation from nonlinear effects. It is noted that higher output power was available from this amplifier when operating with longer pulses that had reduced peak power, or with the same pulses at higher repetition rates.

A narrow band spectral filter formed by a circulator and FBG follows before the final amplification stage. This ensures a clean seed spectrum entering the power amplifier, which is important for two reasons. Firstly, approximately 2% of the power after the second amplification stage corresponds to ASE at shorter wavelengths. The power amplifier has considerable gain at these wavelengths, which increases this content to ~30% after amplification in the absence of spectral filtering. Secondly, it is important to suppress the light in closer vicinity to the signal wavelength (±10−20 nm) that can act as seed for modulation instability in the power amplifier.

3.3. Power amplifier

After losses in the final spectral filter and the (6+1)x1 pump-signal combiner, 1.1 W at 1950 nm and ~90 mW at 2108 nm enters the tandem power amplifier in Fig. 1. When 790 nm pump light is launched into the thulium fiber, both signals experience gain since the thulium emission band covers both wavelengths. This is seen in the input-output curve measured after the Tm fiber in Fig. 3(a), where the 2108 nm signal is amplified to 0.34 W and the 1950 nm signal to 23 W at the maximum launched pump power of 52 W. Considering only the 1950 nm signal, an optical conversion efficiency of 42% is achieved in the Tm fiber. The Tm gain spectrum becomes blue shifted as the inversion density increases with pump power, thus increasingly favoring amplification at 1950 nm relative to 2108 nm. This effect explains the decreasing slope observed for the 2108 nm signal.
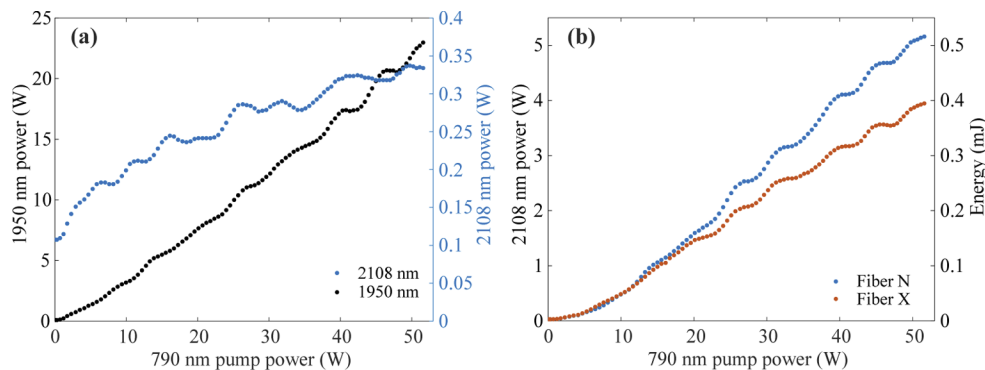

Fig. 3. Output power from the tandem power amplifier after the thulium fiber (a) and after the holmium fibers from two different suppliers (b).

The oscillatory appearance revealed when sampling the power curves densely is attributed to mode-dependent splice losses for the 1950 nm light. The large mode area thulium fiber used (20 μm core, 0.08 NA) has an estimated cut-off wavelength of ~2060 nm, and is hence single mode for the 2108 nm seed-signal, but not at 1950 nm. The oscillations were reproducible and stable in time for a given coiling arrangement, and not investigated further.

Figure 3(b) shows the average output power at 2108 nm measured after the two different holmium fibers that were tested in the tandem amplifier. Maximum average output powers of 4.0 W and 5.2 W are obtained from Fiber X and Fiber N, respectively. Also shown are the corresponding pulse energies inferred from the 10 kHz repetition rate. The amount of unabsorbed

1950 nm pump at maximum power is approximately 2% for both fibers when using the lengths optimized for highest output power in cut-back experiments. A relatively poor slope efficiency of 26% and 16% measured against the 1950 nm pump is seen for the two fibers, compared to a quantum defect limit of 93% for this combination of pump and signal wavelengths.

3.3.1. Spectroscopy and non-saturable absorption

The <30% slope efficiency observed with respect to 1950 nm pump light was unexpected at first because the 2108 nm seed power exceeds the saturation power of the holmium fibers (~ 300 mW), and because the amplifier operates at a repetition rate much higher than the inverse fluorescent lifetime (~ 0.6 ms).

It is speculated that the reduced slope efficiency is related to holmium ion clustering and associated pair induced quenching (PIQ). This is a well-established and thoroughly investigated spectroscopic challenge in erbium-doped fibers [19], and has recently been suggested as the dominant cause of the lower-than-expected efficiency of holmium-doped silica fibers [20–22]. The presence of clusters gives rise to non-saturable absorption, since the very rapid upconversion occurring between ions in immediate vicinity prevents more than one of the ions in a cluster to be excited at any given time [19]. Figure 4(a) shows the measured transmission of 1950 nm light through different lengths of Fiber X in the absence of any 2108 nm signal. A considerable amount of non-saturable absorption is indeed revealed, specifically α_{ns} = 4.8 dB/m as found from the linear fit in Fig. 4(b). Equivalent transmission measurements of Fiber N yield α_{ns} = 3.4 dB/m.
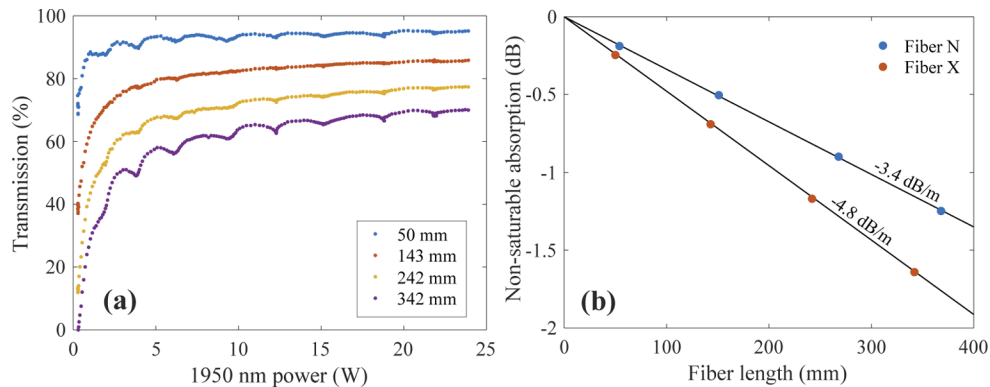

Fig. 4. Transmission of 1950 nm light in different lengths of the Fiber X (IXF-HDF-PM-20-250) (a), and corresponding values for the non-saturable absorption (b) for this fiber and from equivalent measurements of Fiber N (LMA-HDF-25/250).

An estimate of how this measured non-saturable absorption impacts amplifier performance can be obtained following the approach of Le Gouët et al. [22], where the non-saturable absorption is included directly as a loss channel for the 1950 nm light. This approximation is expected to hold reasonably well at the input of the power amplifier, since the input pump power is much higher than the pump saturation power (<0.1 W), while the 2108 nm signal is still relatively low. With this assumption, the amplifier is modeled with rate equations considering only the $^5I_8$–$^5I_7$ transitions, and these numerical simulations suggest indeed output powers that are consistent to within 5% of the experimental results in Fig. 3(b). A more rigorous numerical approach would be that of Wang et al. [21], where the holmium fiber medium was modeled using rate equations that account for PIQ by dividing the holmium population into two species corresponding to single and paired ions. This approach requires detailed knowledge of several uncertain spectroscopic parameters, and such studies fall outside the scope of this work.

It is noted that the measured non-saturable absorption alone explains the obtained efficiencies, irrespective of what its detailed spectroscopic origin might be. Holmium ion clustering nevertheless appears as a likely dominant contributor to the quenching process. Under this assumption, the non-saturable absorption measured in Fig. 4 can be used to determine the fraction of ions residing in pairs through [19]

$$2k = \frac{\alpha_{\mathrm{ns}}}{\alpha_{\mathrm{ss}}} \cdot \frac{2\sigma_{\mathrm{a}} + \sigma_{\mathrm{e}}}{\sigma_{\mathrm{a}}}, \tag{1}$$

where α_{ns} and α_{ss} are the coefficients for non-saturable and small-signal absorption, and σ_{a} and σ_{e} are absorption and emission cross sections. The common notation has been followed where k refers to the relative number of clusters in the fiber, and $2k$ is the fraction of ions that are contained in clusters of two ions, i.e. pairs [19]. Using the measured values of α_{ns} along with $\alpha_{\mathrm{ss}} = 79$ dB/m for Fiber X, $\sigma_{\mathrm{a}} = 4.3 \times 10^{-25}$ m^2 and $\sigma_{\mathrm{e}} = 6 \times 10^{-25}$ m^2 [22], Eq. (1) suggests $2k = 21\%$. In other words, 21% of the holmium ions in Fiber X reside in clusters. For Fiber N ($\alpha_{\mathrm{ss}} = 66$ dB/m), a somewhat lower degree of clustering is inferred at $2k = 17\%$. These measured levels of clustering are comparable to recently reported studies of other holmium fibers with similar concentration [22].

It is concluded that, despite the holmium-doped fibers investigated here being produced by leading manufacturers, the degree of clustering seems considerable, and of a magnitude sufficient to explain the experimental results in Fig. 3(b). Thus, significant improvements in performance primarily motivate efforts to improve doping homogeneity. One potentially promising fabrication strategy in this regard is nanoparticle doping [23]. Still, it is expected that even small amounts of clustered ions will be deleterious for high gain operation. This may be intrinsically challenging to avoid [21], especially in combination with the opposing desire to have a high doping concentration in a pulsed amplifier for reducing device lengths.

Besides efforts to improve spectroscopy, certain modifications to the power amplifier may improve efficiency with the currently available fibers. Primarily, the power efficiency can be increased by operating at a lower gain. In fact, slope efficiencies approaching 60% have been reported in low gain laser/amplifier setups incorporating the two specific fibers used in this work [10,24]. Such setups are suitable for average power scaling, but it is noted that a pulsed system with high peak powers will strongly benefit from having moderate or high gain in the final stage. Reverse pumping of the final holmium fiber is also expected to be advantageous by reducing the inversion level where the pump power is highest. This is however impractical to combine with the tandem architecture of the power amplifier. Finally, it may be beneficial to implement pulsed pumping if the duration of the pump and signal pulses is comparable to or shorter than the lifetime of excited ion pairs. To our knowledge, no such lifetime studies exist for holmium-doped fibers, but a ~50 ns lifetime has been reported for excited erbium pairs [25].

It is noted that another potential contributor to the reduced efficiency in the power amplifier in addition to PIQ could be gain depletion in the Tm fiber caused by reverse ASE generated in the Ho fiber. This is however ruled out from numerical simulations that suggest ~ 120 µW of reverse ASE generated in the Ho fiber. This is orders of magnitude below the 1950 nm and 2108 nm seed signals entering the tandem amplifier, and is not expected to deplete the Tm gain noticeably.

3.3.2. Temporal profiles, optical spectrum and beam quality

Although the moderate slope efficiency limits the average power of the MOPA, high energy pulses with attractive characteristics for ZGP OPO pumping are realized in the current setup. Figure 3(b) shows maximum pulse energies of 0.40 mJ and 0.52 mJ from Fiber X and N, respectively. This corresponds approximately to twice the saturation energy in both fibers, and is therefore expected to be comparable in magnitude to what can be practically extracted from these fibers. Figure 5 shows the temporal profile of the output pulses from Fiber N. There were no detectable

fluctuations in shape or amplitude from pulse to pulse, hence an average of 16 pulses is shown for reducing the sampling noise. A nearly square pulse shape with 50 ns duration and 11 kW peak power is obtained, but the power is seen to drop towards the end of the pulse due to insufficient precompensation of the dynamic gain saturation. Improved squareness could be realized, but was not pursued since it implied weaker seeding and reduced efficiency of the power amplifier. The near square profile in Fig. 5 is an attractive and important feature of the MOPA, as it is ultimately peak power limited from nonlinear effects. Also, square pulses have been shown to be well suited for achieving high conversion efficiency in OPO applications [12,26].
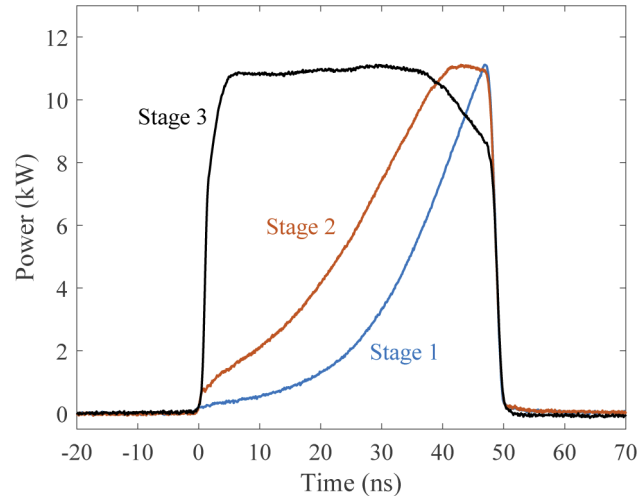

Fig. 5. Temporal pulse profiles measured with a 1 GHz detection bandwidth after different stages in the MOPA. The power scale applies to the pulse from stage 3, while the pulses from stages 1 and 2 have been vertically scaled for comparison purposes. The profile for stage 1 is measured *after* the AOM in Fig. 1.

Figure 6 shows the optical spectrum measured at maximum power from Fiber N. In addition to the signal at 2108 nm, the wide spectrum contains two distinct broadband features corresponding to amplified spontaneous emission peaking at 2020 nm, and symmetric side bands at −40 dB next to the signal attributed to modulation instability (MI). Numerical integration of the optical spectrum reveals that the ASE contributes to less than of 0.8% of the total average power.

The MI spectral features correspond to degenerate four wave mixing that is phase matched via self phase modulation in the anomalously dispersive gain fiber [14]. This process is detrimental in the sense of transferring power into spectral side bands, which depletes the spectral power useful for nonlinear conversion in a ZGP OPO and other applications requiring narrow-band emission. The fraction of power contained within a 1 nm bandwidth in Fig. 6 is 96%. In essence, the spectral broadening starts to become considerable for these pulses, from which it was decided to limit the peak power of the pulses to 10-12 kW. It is noted that shorter pulses with a similar energy but higher peak powers towards 20 kW could also be generated from the MOPA, but operation beyond ∼10 kW was avoided due to degraded output spectra and expected usefulness in the targeted nonlinear conversion application.

The process currently limiting peak power scaling is in other words modulation instability, despite the precautionary design choices incorporated in the MOPA; the final spectral filter ensures a clean seed spectrum launched into the power amplifier, and the length of the final holmium-doped fiber is kept as short as practically possible by utilizing core pumping at the peak absorption wavelength. It is believed that considerable increases in peak power beyond the 11 kW reported here would require transition to alternative gain fibers with increased mode area
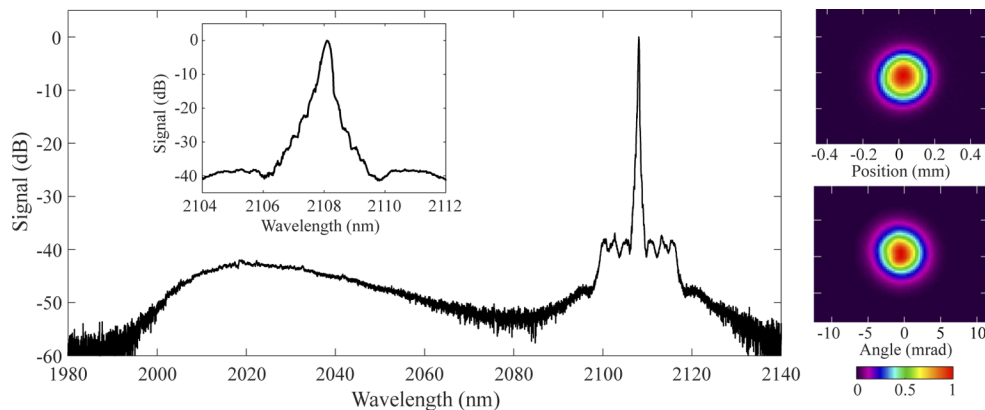
Fig. 6. Optical spectrum at maximum power measured with a resolution of 0.2 nm. The inset shows details around the signal wavelength. Also shown are near- and far field beam profiles of a waist generated after the MOPA.

and/or higher doping concentration. No signs of stimulated Brillouin scattering were seen up to maximum power. This is consistent with the numerical analysis in Section 3.1 where an SBS threshold of 61 kW (3 mJ) was found for 50 ns square pulses with the spectral characteristics measured for the seed pulses.

Also shown in Fig. 6 are beam profiles captured with a pyro-electric camera (Pyrocam III, Spiricon) of a waist and its corresponding far field generated after the MOPA. This waist is used for pumping the ZGP OPO in Section 3.5. An M^2 beam quality of ~1.1 is determined from the second moment waist diameter of 0.35 mm and divergence of 8.1 mrad. Similar near diffraction-limited beam quality is obtained when using Fiber X.

The MOPA output has a measured degree of linear polarization of >95% when using the polarization maintaining Fiber X in the power amplifier. The polarization state fluctuates slowly with time when using the non-PM Fiber N. In practice, the output was still ~90% linearly polarized, and could be further optimized by manually manipulating the fiber. This procedure was found to be acceptable for conducting the OPO-experiments presented in Section 3.5, although a PM-version of Fiber N would be preferred for long term polarization stability.

3.4. MOPA summary

A holmium-based fiber MOPA operating at 2.1 μm has been demonstrated, delivering linearly polarized output of 0.52 mJ at 10 kHz repetition rate, and a nearly square temporal pulse shape with 11 kW peak power. Careful attention to the temporal and spectral quality of the pulses was provided from the pulsed seed diode, through a high-gain front end consisting of two preamplification stages, and to the final tandem power amplification stage. One of the major challenges in scaling the peak power of fiber laser sources is the suppression of nonlinear effects. The diode seeded MOPA is attractive in this regard since it is naturally compatible with temporal and spectral pulse shaping. It is noted that the MOPA flexibility does come at the cost of complexity compared to alternative source architectures such as single oscillator Q-switched fiber lasers [8].

It is argued that the tandem power amplifier architecture in the MOPA has principally attractive features for generating high average power nanosecond pulses in the 2.1 μm-regime. Cladding pumped thulium fibers are relied upon for power scaling, while the following holmium fiber allows amplification at longer wavelengths than practical with Tm only. It is questionable whether the net efficiency of this approach will exceed the possibilities with a single co-doped Tm:Ho

fiber stage. Thermal handling of co-doped Tm:Ho is however challenging at high powers, which motivates separation into two fibers. A tandem amplifier with mode-matched Tm and Ho fibers supports core pumping at principally very high powers, since no challenging requirements are imposed on components such as fused wavelength-division multiplexers used for spectrally combining pump and signal. Core pumping is generally attractive in pulsed sources that benefit from short device lengths, and particularly attractive in holmium amplifiers where in-band cladding pumping cannot be done with conventional polymer-based double clad fibers that absorb in the 2 μm-band.

The average power of the power amplifier is limited by quenching effects in currently available holmium fibers, hindering efficient operation at high gain. Considerable improved spectroscopic properties are required to mitigate this, but may ultimately prove difficult due to the high inversion density required for achieving gain in holmium-doped silica, and thus a sensitivity to even small amounts of clustering. Average power scaling beyond the presented results is still believed to be realistic by introducing an additional amplification stage, which is operated at a low gain. This will be explored in future work, and such an amplifier would be very similar to Yao et al. [10], who reported 99 W average power from a 2.1 μm core pumped tandem amplifier using Fiber N from this work.

3.5. ZnGeP$_2$ optical parametric oscillator

A ZGP OPO was constructed and directly pumped by the MOPA for optical frequency conversion to the mid-IR. The singly resonant OPO setup is shown in Fig. 7(a), which includes details about the components used. The pump beam is shown in Fig. 6, and had a $1/e^2$ diameter of 0.35 mm. The 13.5 mm ZGP crystal was AR-coated and cut at an angle of 54° with respect to the c-axis for Type I phase matching. A V-resonator with three plane mirrors previously developed in our group was used [3], and components were chosen on the basis of numerical simulations with in-house simulation software for nonlinear interactions and lasers (SISYFOS). This resonator has attractive features such as two pump passes in a single crystal while eliminating pump feedback, the two beams don't overlap in the crystal which both enhances the damage threshold and reduces the impact of thermal effects, and a fairly short round-trip can be realized easily (here: 57 mm).
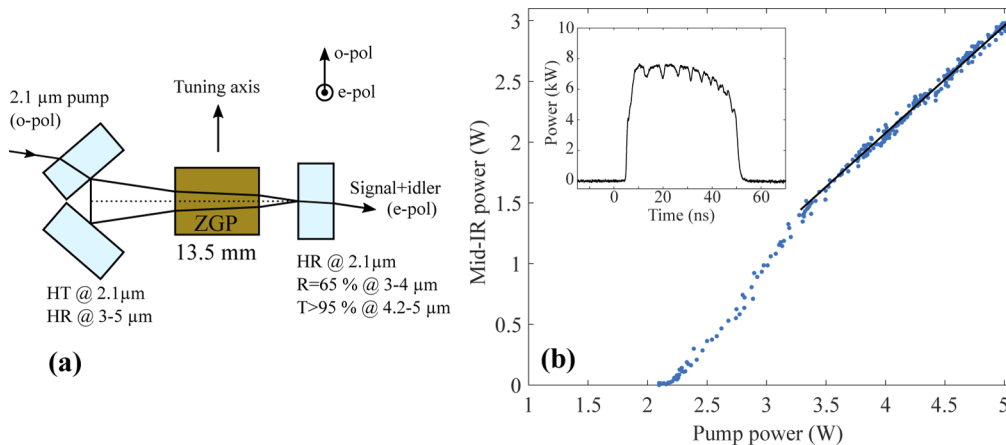

Fig. 7. Illustration of the OPO setup (a) and measured mid-infrared output power (b). The inset in (b) shows the mid-IR pulse profile.

Figure 7(b) shows the measured mid-IR power (3.9 μm signal + 4.6 μm idler) for pump powers that were adjusted by attenuating the MOPA output with a half wave plate and polarizer. Since the polarization of the MOPA drifted slightly with time when using the non-polarization maintaining

Fiber N, the OPO output power and the launched pump power at the OPO in-coupling mirror were recorded simultaneously. A kink is seen in the power curve at an output power of ~1.5 W. The high slope observed below this point is explained by the OPO build-up time reducing with pump power so that an increasing fraction of the pump pulse becomes available for conversion. It was verified that the kink corresponded to the point at which the build-up time (~5 ns) had been reduced to a small fraction of the pump duration and was therefore not significantly further reduced with increasing pump power. The solid line in Fig. 7(b) corresponds to a linear fit with a slope of 0.88. The inset in Fig. 7(b) shows the temporal output profile at maximum power, which reveals a modulation pattern that was reproduced in numerical simulations and is attributed to the frequency evolution of the pump pulse. An M^2 beam quality of 1.7 (signal) and 2.1 (idler) was determined at maximum output power based on measurements of second moment diameters of waist and far field beam profiles.

A mid-IR output of 3.0 W is obtained at the maximum launched pump power of 5.1 W. This corresponds to a conversion efficiency of 59%, which is considerably higher than previously reported ZGP OPOs pumped by various types of fiber-based sources (15% to 32% [4–8]). This improvement is attributed to the application-tailored features of this MOPA; the long ~2.1 μm pump wavelength (low ZGP absorption), square pulse shape, high peak power, high pulse energy and good spectral and spatial beam quality. Furthermore, a remarkable stability is experienced in both temporal profile and energy from pulse to pulse from the OPO, which is inherited from the spectral and temporal stability the MOPA.

It is believed that the operational flexibility and stability of the MOPA pulses can be exploited for OPO optimization. This will be the explored in future work, particularly in terms of prospects for average power scaling.

4.   Conclusion

An alignment-free holmium-doped fiber amplifier with three stages has been demonstrated, delivering 0.52 mJ pulses at 10 kHz repetition rate at a wavelength of 2108 nm with near diffraction-limited beam quality and linear polarization. The output pulses are shaped to a square temporal profile of 50 ns duration and 11 kW peak power, and the shaping also introduces a frequency shift through the pulse that suppresses stimulated Brillouin scattering. The slope efficiency of the final stage amplifier is found to be only ~20% using holmium fibers from two different manufacturers. This is explained by measurements that show substantial non-saturable absorption in both fibers, which may again be attributed to Ho-ion clustering and pair-induced quenching. Despite the moderate efficiency and average power currently achieved, the output pulses are of high quality and appear suitable for optical frequency conversion to the mid-IR. Preliminary experiments demonstrate a conversion efficiency to the mid-IR of 59% when directly pumping a ZnGeP$_2$ optical parametric oscillator, which indicates substantial mid-IR average power scaling potential of ZGP OPOs pumped by fiber-based sources.

References

1.   A. Hemming, N. Simakov, J. Haub, and A. Carter, "A review of recent progress in holmium-doped silica fibre sources," Opt. Fiber Technol. **20**(6), 621–630 (2014).
2.   P. Schunemann, K. Zawilski, L. Pomeranz, D. Creeden, and P. Budni, "Advances in nonlinear optical crystals for mid-infrared coherent sources," J. Opt. Soc. Am. B **33**(11), D36–D43 (2016).
3.   E. Lippert, H. Fonnum, G. Arisholm, and K. Stenersen, "A 22-watt Mid-infrared optical parametric oscillator with V-shaped 3-mirror ring resonator," Opt. Express **18**(25), 26475–26483 (2010).
4.   C. Kieleck, A. Berrou, B. Donelan, B. Cadier, T. Robin, and M. Eichhorn, "6.5 W ZnGeP$_2$ OPO directly pumped by a Q-switched Tm^{3+}-doped single-oscillator fiber laser," Opt. Lett. **40**(6), 1101–1104 (2015).

5. D. Creeden, P. Ketteridge, P. Budni, S. Setzler, Y. Young, J. McCarthy, K. Zawilski, P. Schunemann, T. Pollak, E. Chicklis, and M. Jiang, "Mid-infrared ZnGeP$_2$ parametric oscillator directly pumped by a pulsed 2 μm Tm-doped fiber laser," Opt. Lett. **33**(4), 315–317 (2008).
6. N. Simakov, A. Davidson, A. Hemming, S. Bennetts, M. Hughes, N. Carmody, P. Davies, and J. Haub, "Mid-infrared generation in ZnGeP$_2$ pumped by a monolithic, power scalable 2 μm source," Proc. SPIE **8237**, 82373K (2012).
7. M. Gebhardt, C. Gaida, P. Kadwani, A. Sincore, N. Gehlich, C. Jeon, L. Shah, and M. Richardson, "High peak-power mid-infrared ZnGeP^2 optical parametric oscillator pumped by a Tm:fiber master oscillator power amplifier system," Opt. Lett. **39**(5), 1212–1215 (2014).
8. N. Dalloz, T. Robin, B. Cadier, C. Kieleck, M. Eichhorn, and A. H.-Dhollande, "High power Q-switched Tm^{3+}, Ho^{3+}-codoped 2 μm fiber laser and application for direct OPO pumping," Proc. SPIE **10897**, 108970J (2019).
9. A. Hemming, J. Richards, N. Simakov, A. Davidson, N. Carmody, J. Haub, and A. Carter, "Pulsed operation of a resonantly pumped, linearly polarised, large mode area holmium-doped fibre amplifier," Opt. Express **22**(6), 7186–7193 (2014).
10. W. Yao, C. Shen, Z. Shao, Q. Liu, H. Wang, Y. Zhao, and D. Shen, "High-power nanosecond pulse generation from an integrated Tm–Ho fiber MOPA over 2.1 μm," Opt. Express **26**(7), 8841–8848 (2018).
11. N. Simakov, A. Hemming, K. Boyd, A. Davidson, J. Daniel, N. Carmody, R. Swain, E. Mies, M. Oermann, W. A. Clarkson, K. Farley, A. Carter, and J. Haub, "Mitigation of spectral broadening in high peak power holmium-doped fibre sources," in *2017 Conference on Lasers and Electro-Optics Europe & European Quantum Electronics Conference (CLEO/Europe-EQEC)*, (2017), pp. 1.
12. G. Aoust, A. Godard, M. Raybaut, O. Wang, J.-M. Melkonian, and M. Lefebvre, "Optimal pump pulse shapes for optical parametric oscillators," J. Opt. Soc. Am. B **33**(5), 842–849 (2016).
13. K. Petermann, *Laser diode modulation and noise* (Kluwer Academic Publishers, 1991).
14. G. Agrawal, *Nonlinear Fiber Optics* (Academic Press, 2013), 5th ed.
15. C. Zeringue, I. Dajani, S. Naderi, G. Moore, and C. Robin, "A theoretical study of transient stimulated Brillouin scattering in optical fibers seeded with phase-modulated light," Opt. Express **20**(19), 21196–21213 (2012).
16. J. White, A. Vasilyev, J. Cahill, N. Satyan, O. Okusaga, G. Rakuljic, C. Mungan, and A. Yariv, "Suppression of stimulated Brillouin scattering in optical fibers using a linearly chirped diode laser," Opt. Express **20**(14), 15872 (2012).
17. P. Ionov and T. Rose, "SBS Reduction in nanosecond fiber amplifiers by frequency chirping," Opt. Express **24**(13), 13763–13777 (2016).
18. N. Simakov, Z. Li, Y. Jung, J. Daniel, P. Barua, P. Shardlow, S. Liang, J. Sahu, A. Hemming, W. Clarkson, S.-U. Alam, and D. Richardson, "High gain holmium-doped fibre amplifiers," Opt. Express **24**(13), 13946–13956 (2016).
19. P. Myslinski, D. Nguyen, and J. Chrostowski, "Effects of concentration on the performance of erbium-doped fiber amplifiers," J. Lightwave Technol. **15**(1), 112–120 (1997).
20. J. Wang, D. Yeom, N. Simakov, A. Hemming, A. Carter, S. Lee, and K. Lee, "Numerical modeling of in-band pumped Ho-doped silica fiber lasers," J. Lightwave Technol. **36**(24), 5863–5880 (2018).
21. J. Wang, N. Bae, S. Lee, and K. Lee, "Effects of ion clustering and excited state absorption on the performance of Ho-doped fiber lasers," Opt. Express **27**(10), 14283–14297 (2019).
22. J. Gouët, F. Gustave, P. Bourdon, T. Robin, A. Laurent, and B. Cadier, "Realization and simulation of high power holmium doped fiber laser for long-range transmission," Opt. Express **28**(15), 22307–22320 (2020).
23. C. Baker, E. Friebele, A. Burdett, D. Rhonehouse, J. Fontana, W. Kim, S. Bowman, B. Shaw, J. Sanghera, J. Zhang, R. Pattnaik, M. Dubinskii, J. Ballato, C. Kucera, A. Vargas, A. Hemming, N. Simakov, and J. Haub, "Nanoparticle doping for high power fiber lasers at eye-safer wavelengths," Opt. Express **25**(12), 13903–13915 (2017).
24. E. Lallier, "30 W gain-switched holmium-doped fiber laser at 2.09 μm," OPTRO 2020 **059** (2020).
25. P. Myslinski, J. Fraser, and J. Chrostowski, "Nanosecond kinetics of upconversion process in EDF and its effect on EDFA performance," in *Optical Amplifiers and Their Applications*, (Optical Society of America, 1995), p. ThE3.
26. Z. Sacks, O. Gayer, E. Tal, and A. Arie, "Improving the efficiency of an optical parametric oscillator by tailoring the pump pulse shape," Opt. Express **18**(12), 12669–12674 (2010).